

Pion, Kaon and Antiproton Production in $Pb + Pb$ Collisions at LHC Energy $\sqrt{s_{NN}} = 2.76$ TeV : A Model-based Analysis

P. Guptaroy^{1,*}, S. Guptaroy^{2,†}

¹ Department of Physics, Raghunathpur College,
P.O.: Raghunathpur 723133, Dist.: Purulia (WB), India.

² Department of Physics, Basantidevi College,
147B Rashbehari Avenue, Kolkata 700029 India.

Abstract

Large Hadron Collider (LHC) had produced a vast amount of high precision data for high energy heavy ion collision. We attempt here to study (i) transverse momenta spectra, (ii) K/π , p/π ratio behaviours, (iii) rapidity distribution, and (iv) the nuclear modification factors of the pion, kaon and antiproton produced in $p + p$ and $Pb + Pb$ collisions at energy $\sqrt{s_{NN}} = 2.76$ TeV, on the basis of Sequential Chain Model (SCM). Comparisons of the model-based results with the measured data on these observables are generally found to be modestly satisfactory.

Keywords: Relativistic heavy ion collisions, baryon production, light mesons

PACS nos.: 25.75.-q, 13.60.Rj, 14.40.Be

*e-mail: gpradeepta@gmail.com (Communicating author)

†e-mail: simaguptaroy@yahoo.com

1 Introduction

Heavy ion collisions at ultra relativistic energies might produce a new form of QCD matter characterized by the deconfined state of quarks and gluons (partons) [1]. Measurements of the production of identified particles provide information about the dynamics of this dense matter. The yield of identified hadrons, their multiplicity distributions, as well as the rapidity and transverse momentum spectra are the basic observables in proton-proton and heavy ion collisions at any energy regime, from a few GeV per nucleon to the new ultra-relativistic LHC regime, spanning c.m. energies of a few TeV.[2] Recently, experimental results in $Pb + Pb$ collisions at $\sqrt{s_{NN}} = 2.76$ TeV in the Large Hadron Collider (LHC) are also reported by the different groups. These results might provide another opportunity to investigate the bulk properties of exotic QCD matter, the so-called QGP-hypothesis. But the exact nature of QGP- hadron phase transition is still plagued by uncertainties.[3]

Our objective in this work is to use a model, known as ‘Sequential Chain Model (SCM)’, which is different from ‘standard’ framework, in interpreting the transverse momenta spectra, some ratio-behaviours, rapidity spectra and the nuclear modification factor of the pions, kaons and antiprotons for $p + p$ and $Pb + Pb$ collisions at LHC energy $\sqrt{s_{NN}} = 2.76$ TeV. Very recently, a question has been raised about the quark-gluon composition of proton.[4] So, in order to explain the huge amount of heavy ion collision data, we put forward this model which has no QGP-tag and is different from the quark-hypothesis.

The organization of this work is as follows. In section 2 we give a brief outline of our approach, the SCM. In the next section (section 3) the results arrived at have been presented with table and figures. And in the last section (section 4) we offer the final remarks and conclusions.

2 Outline of the Model

This section is divided by two subsections (1) the basic model in $p+p$ collision and (2) subsequent transformation to the $A + B$ collisions.

2.1 The Basic Model: An Outline

According to this Sequential Chain Model (SCM), high energy hadronic interactions boil down, essentially, to the pion-pion interactions; as the protons are conceived in this model as $p = (\pi^+ \pi^0 \vartheta)$, where ϑ is a spectator particle needed for the dynamical generation of quantum numbers of the nucleons.[5]-[11]

The inclusive cross-section of the π^- -meson produced in the $p + p$ collisions at high energies has been calculated by using field theoretical calculations and Feynman diagram techniques with the infinite momentum frame approximation method. The inclusive cross-section is given by the undernoted relation [5]-[11]

$$E \frac{d^3\sigma}{dp^3} |_{pp \rightarrow \pi^- x} \cong \Gamma_{\pi^-} \exp(-2.38 \langle n_{\pi^-} \rangle_{pp} x) \frac{1}{p_T^{(N_R^{\pi^-})}} \exp\left(\frac{-2.68 p_T^2}{\langle n_{\pi^-} \rangle_{pp} (1-x)}\right), \quad (1)$$

with

$$\langle n_{\pi^+} \rangle_{pp} \cong \langle n_{\pi^-} \rangle_{pp} \cong \langle n_{\pi^0} \rangle_{pp} \cong 1.1 s^{1/5}, \quad (2)$$

where Γ_{π^-} is the normalisation factor which will increase as the inelastic cross-section increases and it is different for different energy region and for various collisions. The terms p_T , x

$[x \simeq 2p_{zcm}/\sqrt{s} = 2m_T \sinh y_{cm}/\sqrt{s}]$ in equation (1) represent the transverse momentum, Feynman Scaling variable respectively. The s in equation (2) is the square of the c.m. energy.

$1/p_T^{N_R^-}$ of the expression (1) is the ‘constituent rearrangement term’. It arises out of the partons inside the proton. At high energy interaction processes the partons undergo some dissipation losses due to impact and impulses of the projectile on the target. This term essentially provides a damping term in terms of a power law. The exponent of p_T , i.e. N_R , varies on both the collision process and the specific p_T -range. We have to parametrize this term with the view of two physical points, viz., the amount of momentum transfer and the contributions from a phase factor arising out of the rearrangement of the constituent partons. The relation for N_R is to be given by [12]

$$N_R = 4 < N_{part} >^{1/3} \theta, \quad (3)$$

where $< N_{part} >$ denotes the average number of participating nucleons and θ values are to be obtained phenomenologically from the fits to the data-points.

Similarly, for kaons of any specific variety (K^+ , K^- , K^0 or \bar{K}^0) we have

$$E \frac{d^3\sigma}{dp^3} |_{pp \rightarrow K^- x} \cong \Gamma_{K^-} \exp(-6.55 < n_{K^-} >_{pp} x) \frac{1}{p_T^{(N_R^{K^-})}} \exp\left(\frac{-1.33 p_T^2}{< n_{K^-} >_{pp}^{3/2}}\right), \quad (4)$$

with

$$< n_{K^+} >_{pp} \cong < n_{K^-} >_{pp} \cong < n_{K^0} >_{pp} \cong < n_{\bar{K}^0} >_{pp} \cong 5 \times 10^{-2} s^{1/4}. \quad (5)$$

And for the antiproton production in pp collision at high energies, the derived expression for inclusive cross-section is

$$E \frac{d^3\sigma}{dp^3} |_{pp \rightarrow \bar{p} x} \cong \Gamma_{\bar{p}} \exp(-25.4 < n_{\bar{p}} >_{pp} x) \frac{1}{p_T^{(N_R^{\bar{p}})}} \exp\left(\frac{-0.66((p_T^2)_{\bar{p}} + m_{\bar{p}}^2)}{< n_{\bar{p}} >_{pp}^{3/2} (1-x)}\right), \quad (6)$$

with

$$< n_{\bar{p}} >_{pp} \cong < n_p >_{pp} \cong 2 \times 10^{-2} s^{1/4}, \quad (7)$$

2.2 The Path from pp to AB Collisions

In order to transform the inclusive cross-section from $pp \rightarrow C^- + X$ to $AB \rightarrow C^- + X$ collisions (here, C^- stands for π^- , K^- and \bar{p} , as the case may be), we use the undernoted relation; [13]

$$E \frac{d^3\sigma}{dp^3} |_{AB \rightarrow C^- + X} \cong \frac{(A\sigma_B + B\sigma_A)}{\sigma_{AB}} \frac{1}{1 + a'(A^{1/3} + B^{1/3})} E \frac{d^3\sigma}{dp^3} |_{pp \rightarrow C^- + X}, \quad (8)$$

Here, in the above equation [eqn.(8)], the first factor gives a measure of the number of wounded nucleons i.e. of the probable number of participants, wherein $A\sigma_B$ gives the probability cross-section of collision with ‘ B ’ nucleus (target), had all the nucleons of A suffered collisions with B -target. And $B\sigma_A$ has just the same physical meaning, with A and B replaced. Furthermore, σ_A is the nucleon(proton)-nucleus(A) interaction cross-section, σ_B is the inelastic nucleon(proton)-nucleus(B) reaction cross-section and σ_{AB} is the inelastic AB cross-section for the collision of nucleus A and nucleus B . The values of σ_{AB} , σ_A , σ_B have been worked here out by the following formula [14]

$$\sigma_{AB}^{inel} = \sigma_0 (A_{projectile}^{1/3} + A_{target}^{1/3} - \delta)^2 \quad (9)$$

with $\sigma_0 = 68.8$ mb, $\delta = 1.32$.

The second term in expression (8) is a physical factor related with energy degradation of the secondaries due to multiple collision effects. The parameter a' occurring in this term is a measure of the fraction of the nucleons that suffer energy loss. The maximum value of a' is unity, while all the nucleons suffer energy loss. This a' parameter is usually to be chosen [13], depending on the centrality of the collisions and the nature of the secondaries.

3 The Results

This section will be divided in the following sub-sections: (i) the p_T -spectra of pion, kaon and antiproton in both $p + p$ and $Pb + Pb$ collisions at $\sqrt{s_{NN}} = 2.76$ TeV; (ii) K/π and p/π ratio behaviour at $Pb + Pb$ collisions at $\sqrt{s_{NN}} = 2.76$ TeV; (iii) rapidity distribution of pion for the most central collisions of $Pb + Pb$ in the above-mentioned energy and (iv) the nuclear modification factor R_{AA} in the same energy range.

3.1 Transverse Momenta Spectra of Charged Hadron in $p + p$ and $Pb + Pb$ Collision at $\sqrt{s_{NN}} = 2.76$ TeV

We can write from expression (8), the transformed SCM-based transverse-momentum distributions for $A + B \rightarrow C^- + X$ -type reactions in the following generalized notation:

$$\frac{1}{2\pi p_T} \frac{d^2 N}{dp_T dy} \Big|_{A+B \rightarrow C^- + x} = \alpha_{C^-} \frac{1}{N_R^{C^-}} \exp(-\beta_{C^-} \times p_T^2). \quad (10)$$

Where, for example, the parameter α_{π^-} can be written in the following form:

$$\alpha_{\pi^-} = \frac{(A\sigma_B + B\sigma_A)}{\sigma_{AB}} \frac{1}{1 + a(A^{1/3} + B^{1/3})} \Gamma_{\pi^-} \exp(-2.38 < n_{\pi^-} >_{pp} x) \quad (11)$$

In a similar way, the values of β_{π^-} of the equation (10) have been calculated with the help of eqn.(1), eqn.(2). The values of α_{K^-} , $\alpha_{\bar{p}}$, β_{π^-} and $\beta_{\bar{p}}$ have been calculated accordingly by using eqns. (4)- (8). Moreover, for calculation for transverse momenta distribution of antiproton production, the the exponential part will be $\exp(-\beta_{\bar{p}}(p_T^2 + m_{\bar{p}}^2))$ ($m_{\bar{p}} \sim 938 \text{ MeV}/c^2$).

$N_R^{C^-}$ of the expression (10) have been calculated by using eqn. (3).

3.1.1 Production of π^- , K^- and \bar{p} in $p + p$ Collision at $\sqrt{s_{NN}} = 2.76$ TeV

In table 1, the calculated values of α , N_R and β of eqn.(10) for π^- , K^- and \bar{p} have been given.

In figure (1), we have drawn the invariant yields against p_T for π^- , K^- and \bar{p} . By using equation (10) and Table 1 we have plotted the solid lines against the experimental background [15]. The dotted lines in the Fig. show PYTHIA-based results [15].

3.1.2 Invariant Yields of π^- , K^- and \bar{p} in $Pb + Pb$ -Collision at $\sqrt{s_{NN}} = 2.76$ TeV

In a similar fashion, the invariant yields of π^- , K^- and \bar{p} in $Pb + Pb$ collision at LHC energy $\sqrt{s_{NN}} = 2.76$ TeV for different centralities have been plotted in Fig.2(a), 2(b) and 2(c) respectively. The solid lines in the Fig. are the theoretical SCM results while the points show the experimental values.[16]. The values of α_{C^-} , $N_R^{C^-}$ and β_{C^-} of eqn.(10) for pion, kaon and antiproton and for different centralities have been given in Table 2.

3.2 The K/π and p/π ratios

The model-based K/π and p/π ratios as a function of p_T at energies $\sqrt{s_{NN}} = 2.76$ TeV have been obtained from the expression (10), Table 1 and Table 2. Data in Figs. 3(a) and 3(b), for different centralities, viz., for 0-5%, 20-30% and 70-80%, are taken from Ref. [16]. Lines in the Figure show the theoretical plots.

3.3 The Rapidity Distribution

For the calculation of rapidity distribution, we can make use of the following standard relation [17],

$$\frac{dN}{dy} = \frac{1}{\sigma_{in}} \int [E \frac{d^3\sigma}{dp^3}] d^2p_T \quad (12)$$

By using eqn. (1), eqn. (8), Table 2 and eqn. (12), we arrive at the SCM-based rapidity distribution, which is given hereunder;

$$\frac{dN}{dy} = 1895 \exp(-0.025 \sinh y_{cm}). \quad (13)$$

The y_{cm} of the above eqn. (eqn.(13)) has come from $\exp(-2.38 < n_{\pi^-} > x)$ of eqn. (11) with $x = 2m_T \sinh y_{cm}/\sqrt{s}$.

In Fig.4, we have plotted theoretical dN/dy versus y with the help of above equation [eqn. (13)] against experimental background [18]. The dotted line in this Fig. shows the Gaussian fit [18].

3.4 The Nuclear Modification Factor

The nuclear modification factor (NMF) R_{AA} is defined as ratio of charged particle yield in $Pb + Pb$ to that in $p + p$, scaled by the number of binary nuclear collisions $< N_{coll} >$ [19] and is given hereunder

$$R_{AA}(p_T) = \frac{(1/N_{evt}^{AA}) d^2 N_{ch}^{AA} / dp_T d\eta}{< N_{coll} > (1/N_{evt}^{pp}) d^2 N_{ch}^{pp} / dp_T d\eta}, \quad (14)$$

where $< N_{coll} >$ is related with the average nuclei thickness function ($< T_{AA} >$) by the following relation [19]

$$< N_{coll} > = < T_{AA} > \sigma_{pp}^{incl}. \quad (15)$$

Here, σ_{pp}^{incl} is the total inelastic cross section of $p + p$ interactions.

The $d^2 N / dp_T d\eta$ is related to $d^2 N / dp_T dy$ by the following relation:[13]

$$\frac{d^2 N}{dp_T d\eta} = \sqrt{1 - \frac{m^2}{m_T^2 \cosh^2 y}} \frac{d^2 N}{dp_T dy}. \quad (16)$$

In the region, $y \gg 0$, $\frac{d^2 N}{dp_T d\eta} \sim \frac{d^2 N}{dp_T dy}$.

The SCM-based results on NMF's for π^- , K^- and \bar{p} in central $Pb + Pb$ collisions at energies $\sqrt{s_{NN}} = 2.76$ TeV are deduced on the basis of Eqn.(10), Table 1 and Table 2. The equations in connection with $(R_{AA})_{\pi^-}$, $(R_{AA})_{K^-}$ and $(R_{AA})_{\bar{p}}$ are give by the following relations and they are plotted in Fig.5 against p_T . The solid lines in the figure show the theoretical results, while the points show the experimentally measured results [20];

$$(R_{AA})_{\pi^-} = 0.35 p_T^{0.33}, \quad (17)$$

$$(R_{AA})_K = 0.40p_T^{0.73}, \quad (18)$$

$$(R_{AA})_{\bar{p}} = 0.25p_T^{1.33}. \quad (19)$$

4 Discussions and Conclusions

Let us now make some comments on the results arrived at and shown by the diagrams on the case-to-case basis.

(1) The invariant yields against transverse momenta (p_T) for π^- , K^- and \bar{p} in proton-proton collisions obtained on the basis of the SCM are shown in Figure 1. Except for very low- p_T region, there is a bit degree of success. The model disagrees in the low- p_T region. This is due to the fact that the model has turned essentially into a mixed one with the inclusion of power law due to the inclusion of partonic rearrangement factor. However, the power-law part of the equation might not be the only factor for this type of discrepancy. The initial condition and dynamical evolution in heavy-ion collisions are more complicated than we expect. Till now, we do not know the exact nature of reaction mechanism. One might take into account some other factors like radial flow or thermal equilibrium.

(2) Similarly, in calculating the yields for different transverse momenta and for different centralities for π^- , K^- and \bar{p} in lead-lead collisions, we use eqns. (8), (9) and (10) alongwith eqns. (1)-(7). The results are given in Table 2 and are depicted in Figs. 2(a), 2(b) and 2(c) respectively. The top-most curves are for central collisions (0-5%) and the lowest curves are peripheral ones (80-90%). In between these two curves, other centralities (5-10%, 10-20%, 20-30%, 30-40%, 40-50%, 50-60%, 60-70% and 70-80%) have been plotted. For the production of pions, the SCM-based results show good fits from central to peripheral collision. Slight disagreements observed at very low- p_T regions for kaons and protons at central collisions. These are due to the power law part of the model. Here, we see that the constituent rearrangement terms are clearly centrality dependent. This explanation is also true for low- p_T region data in $p + p$ collision.

(3) The K/π and p/π ratio behaviours for different centralities are calculated in the light of the SCM and they are plotted in Figs. 3(a) and 3(b) respectively. The theoretical K/π ratio behaviours are in good agreement with experimental values. Some disagreement are observed in central p/π - ratio in low- p_T regions.

(4) In explaining the rapidity distribution for production of pions (Figure 4), the majority of the produced secondaries, the model works agreeably with data. The comparison with Gaussian fit is satisfactory.

(5) The nuclear modification factors for pion, kaon and proton for central $Pb + Pb$ -collisions for different transverse momenta have been calculated and they are plotted in Figure 5. While the theoretical plots are agreeable in low- p_T regions, they disagree in high- p_T .

Now, let us sum up our observations in the following points; (1) the model under consideration here explains the data modesly well on $Pb + Pb$ collisions at $\sqrt{s_{NN}} = 2.76$ TeV. (2) The particle production in heavy ion collisions can be viewed alternatively by this Sequential Chain Model.

Acknowledgements

The work is supported by University Grants Commission, India, against the order no. PSW-30/12(ERO) dt.05 Feb-13.

References

- [1] B. Abelev et al., [ALICE Collaboration], arXiv:1401.1250v2 [nucl-ex] (16 May 2014).
- [2] F. Riggi, J. Phys. (Conference Series) **424**, 012004 (2013).
- [3] S. Zhang , L. X. Han , Y. G. Ma , J. H.Chen and C. Zhong, Phys. Rev C**89**, 034918 (2014).
- [4] D. de Florian et al., Phys. Rev. Letts. **113**, 012001 (2014).
- [5] P. Guptaroy, S. Guptaroy, Chin. Phys. Letts, **31**, 082501, (2014); [arXiv:1406.6296v1 [hep-ph] 24 Jun 2014].
- [6] P. Guptaroy, Goutam Sau, & S. Bhattacharyya, J. of Mod. Phys., **3**, 116 (2012); [arXiv:1110.6612 v1 [hep-ph] 30 Oct 2011].
- [7] P. Guptaroy, G. Sau, S. K. Biswas, S. Bhattacharyya, IL Nuovo Cimento B **125**, 1071 (2010); [arXiv:0907.2008 v2 [hep-ph] 4 Aug 2010].
- [8] P. Guptaroy, Bhaskar De, G. Sau, S. K. Biswas, S. Bhattacharyya, Int. J. Mod. Phys. A **28**, 5121 (2007).
- [9] P. Bandyopadhyay and S. Bhattacharyya, IL Nuovo Cimento A**43**, 305 (1978).
- [10] S. Bhattacharyya, IL Nuovo Cimento C**11**, 51 (1988).
- [11] S. Bhattacharyya, J. Phys. G**14**, 9 (1988).
- [12] P. Guptaroy, G. Sau, S. K. Biswas, S. Bhattacharyya, Mod. Phys. Lett. A **23**, 1031 (2008).
- [13] C. Y. Wong:‘Introduction to High-Energy Heavy Ion Collisions’ (World Scientific,1994).
- [14] M. C. Abreu et al., NA50 Collaboration Preprint, 15 Feb., 2002 CERN-EP/2002-017
- [15] S. Chatrchyan et al., [CMS Collab.] Eur. Phys. J. C**72**, 2164 (2012).
- [16] B. Abelev et al., [ALICE Collab.] Phys. Rev. C**88**, 044910 (2013).
- [17] A. B. Kaidalov, K. A. Ter-Martirosyan, Sov. J. Nucl. Phys. **36**, 979 (1984).
- [18] B. Abelev et al., [ALICE Collaboration], Phys. Lett. B **726**, 610 (2013).[arXiv:1304.0347v2 [nucl-ex] 27 Jul 2013].
- [19] J. Otwinowski, PoS ConfinementX, 170 (2012); [arXiv:1301.5285v1 [hep-ex] (22 Jan 2013)].
- [20] M. Chojnacki for the ALICE Collaboration, J. Phys.: Conf. Series **509**, 012041 (2014).

Table 1: Values of α , N_R and β for pions, kaons, antiproton and proton productions in $p + p$ collisions at $\sqrt{s_{NN}} = 2.76$ TeV

$(\alpha_{\pi^-})_{pp}$	$(N_R^{\pi^-})_{pp}$	$(\beta_{\pi^-})_{pp}$
0.581	2.163	0.30
$(\alpha_{K^-})_{pp}$	$(N_R^{K^-})_{pp}$	$(\beta_{K^-})_{pp}$
0.165	1.454	0.180
$(\alpha_{\bar{p}})_{pp}$	$(N_R^{\bar{p}})_{pp}$	$(\beta_{\bar{p}})_{pp}$
0.105	1.573	0.180

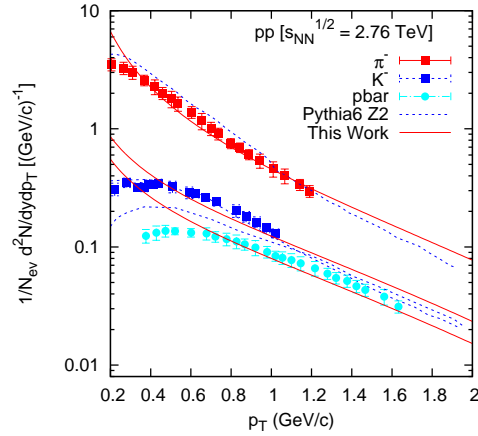


Figure 1: Plots for π^- , K^- , \bar{p} and p productions in $p + p$ collisions at energies $\sqrt{s_{NN}} = 2.76$ TeV. Data are taken [15]. Solid lines in the Figures show the SCM-based theoretical plots while the dotted ones show PYTHIA-based results [15].

Table 2: Values of $(\alpha)_{PbPb}$, $(N_R)_{PbPb}$ and $(\beta)_{PbPb}$ for different centralities for the π^- , K^- and \bar{p} productions in $Pb + Pb$ collisions at $\sqrt{s_{NN}}=2.76$ TeV

Centrality	$(\alpha_{\pi^-})_{PbPb}$	$(N_R^{\pi^-})_{PbPb}$	$(\beta_{\pi^-})_{PbPb}$
0-5%	5.8×10^4	2.493	0.30
5-10%	2.5×10^4	2.483	0.30
10-20%	8.5×10^3	2.472	0.30
20-30%	2.5×10^3	2.464	0.30
30-40%	6.8×10^2	2.456	0.30
40-50%	2.5×10^2	2.444	0.30
50-60%	48	2.434	0.30
60-70%	9.1	2.415	0.30
70-80%	1.8	2.397	0.30
80-90%	0.45	2.392	0.30
Centrality	$(\alpha_{K^-})_{PbPb}$	$(N_R^{K^-})_{PbPb}$	$(\beta_{K^-})_{PbPb}$
0-5%	6.3×10^3	3.314	0.180
5-10%	3.1×10^3	3.015	0.180
10-20%	7.4×10^2	2.784	0.180
20-30%	1.8×10^2	2.583	0.180
30-40%	46	2.321	0.180
40-50%	12	2.124	0.180
50-60%	3.2	2.111	0.180
60-70%	0.62	2.104	0.180
70-80%	0.14	2.008	0.180
80-90%	0.034	1.984	0.180
Centrality	$(\alpha_{\bar{p}})_{PbPb}$	$(N_R^{\bar{p}})_{PbPb}$	$(\beta_{\bar{p}})_{PbPb}$
0-5%	3.1×10^3	3.114	0.180
5-10%	8.4×10^2	2.723	0.180
10-20%	2.6×10^2	2.534	0.180
20-30%	66	2.302	0.180
30-40%	23	2.286	0.180
40-50%	5.9	2.234	0.180
50-60%	1.5	2.201	0.180
60-70%	0.43	2.194	0.180
70-80%	0.072	2.075	0.180
80-90%	0.012	2.034	0.180

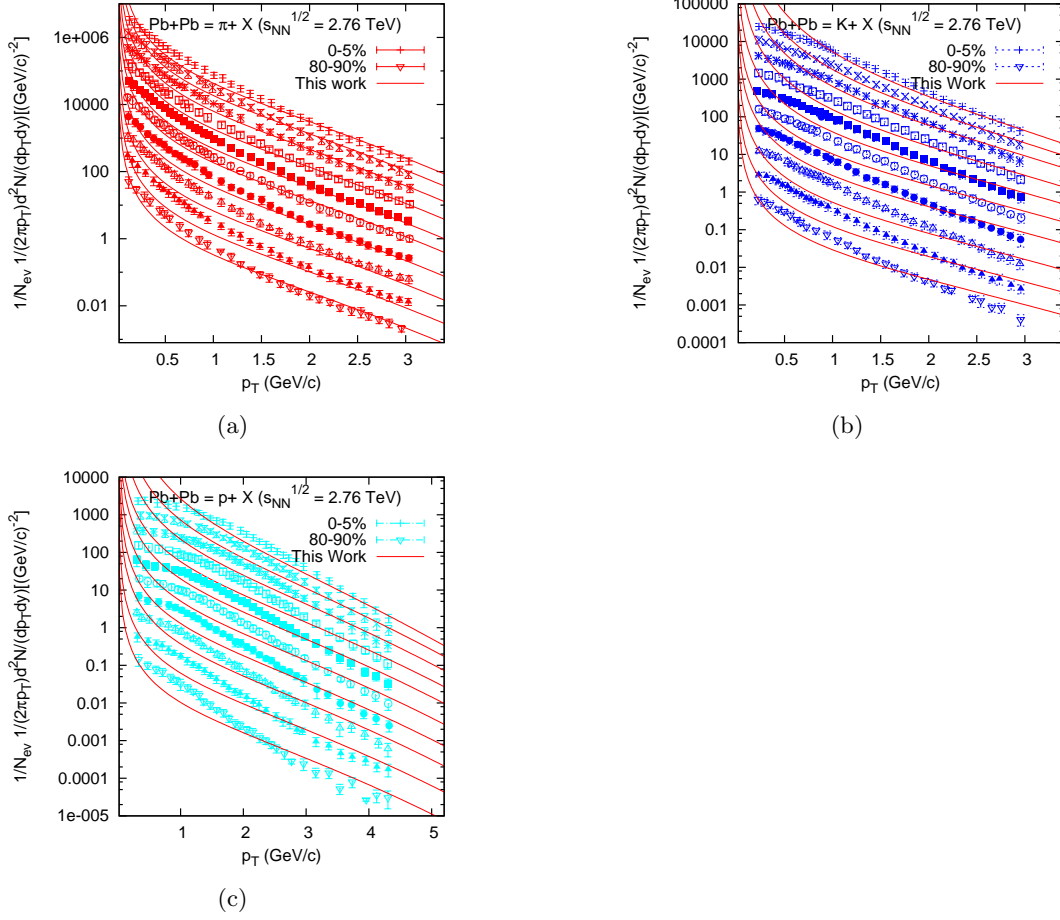


Figure 2: Centrality dependence of the p_T distribution for (a) π^- , (b) K^- and (c) \bar{p} for different centralities in $Pb+Pb$ collisions at energies $\sqrt{s_{NN}} = 2.76$ TeV. Data are taken from [16]. The solid lines in the Figures 2(a), 2(b) and 2(c) show the SCM calculations for different centralities.

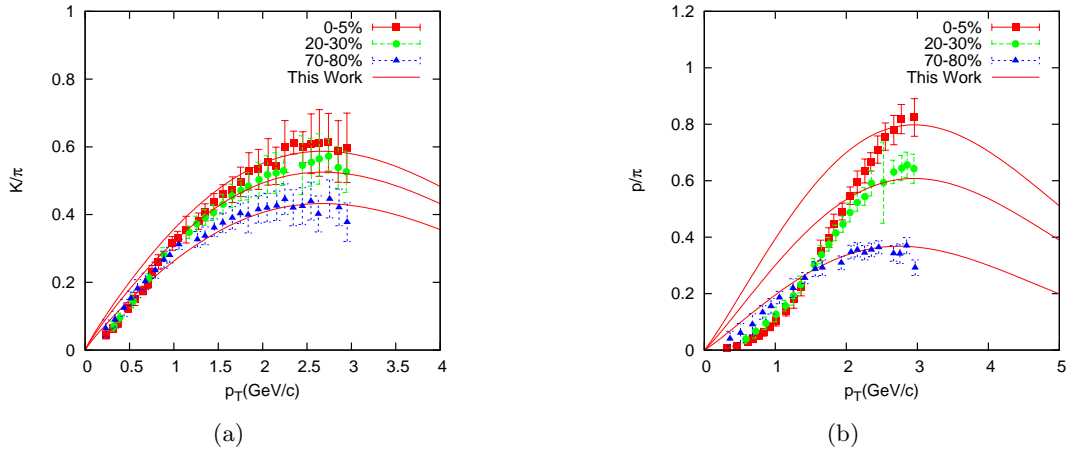


Figure 3: Ratios of (a) K/π and (b) p/π as a function p_T for 0-5%, 20-30% and 70-80% $Pb+Pb$ reactions at $\sqrt{s_{NN}} = 2.76$ TeV. Data in these Figures are taken from [16]. The solid lines show the SCM-based results.

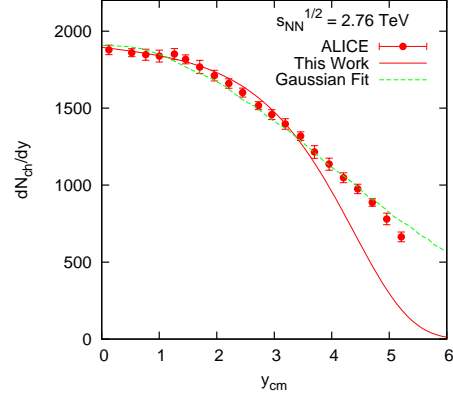


Figure 4: Plot of rapidity distribution of π in central $Pb + Pb$ reactions at $\sqrt{s_{NN}} = 2.76$ TeV. Data in the Figure are taken from [18]. The solid line shows the SCM-based results while the dotted line depicts the Gaussian fit[18].

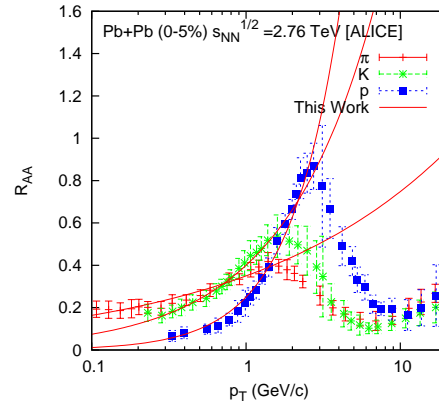


Figure 5: Plots for R_{AA} versus p_T in central $Pb + Pb$ collisions at energies $\sqrt{s_{NN}} = 2.76$ TeV. Data are taken from Ref. [20]. Solid lines in the Figure show the SCM-based theoretical plots.